SIMULATIONS OF TRANSIENT PHENOMENA IN LIQUID ROCKET FEED SYSTEMS

V. Ahuja, A. Hosangadi and P.A. Cavallo
Combustion Research and Flow Technology, Inc. (CRAFT Tech)
Pipersville, PA
and

R. Daines
Jacobs Sverdrup NASA Test Operations Group
NASA Stennis Space Center, MS 39529

ABSTRACT

Valve systems in rocket propulsion systems and testing facilities are constantly subject to dynamic events resulting from the timing of valve motion leading to unsteady fluctuations in pressure and mass flow. Such events can also be accompanied by cavitation, resonance, system vibration leading to catastrophic failure. High-fidelity dynamic computational simulations of valve operation can yield important information of valve response to varying flow conditions. Prediction of transient behavior related to valve motion can serve as guidelines for valve scheduling, which is of crucial importance in engine operation and testing. Feed components operating in cryogenic regimes can also experience cavitation based instabilities leading to large scale shedding of vapor clouds and pressure oscillations. In this paper, we present simulations of the diverse unsteady phenomena related to valve and feed systems that include valve stall, valve timing studies as well as two different forms of cavitation instabilities in components utilized in the test loop.

INTRODUCTION

Experimental testing of rocket engines and associated test articles are carried out in facilities that have complex flow paths that comprise of a network of valves, pipes, arterial branches, orifices and junctions. The complexity in the flow path often leads to flow induced instabilities caused by a variety of factors including vortex shedding, cavitation, turbulence and flow separation. These pressure fluctuations have the potential to amplify and produce deleterious structural vibrations, and system-wide resonance, thereby affecting the entire test loop. Furthermore, most of the engines and test articles operate in dynamic environments in conjunction with test loop system components. In such complex flow environments it is not uncommon for the system to experience severe pressure fluctuations from the coupling between the test article/engine and the valve and feed systems that comprise the test facility leading to premature shutdown of the tests. Furthermore, such deleterious pressure fluctuations are not limited to rocket engine test facilities and have been observed in feed systems onboard the space shuttle and the Delta 4 launch systems. Cavitation related pressure fluctuations were thought to be largely responsible for pressure fluctuations in the oxidizer feedline of the Delta 4 system leading to spurious sensor readings and the premature shutdown of the RS-68 engine. Large scale pressure fluctuations have also contributed to structural damage such as the cracks observed in the space shuttle liquid hydrogen feed liners.

Valve systems are also constantly subject to dynamic events resulting from the timing of valve motion leading to unsteady fluctuations in mass flow and other flow conditions. Such events may be accompanied by cavity formation, resonance, system vibration, and component failure. Currently most analyses involving valve operation are limited to either obtaining steady state performance-related flow coefficient curves [1] or simplified analysis of surge equations in pipeline systems [1]. These analyses fail to account for the transient coupling between valve motion and flow modulation that is an integral part of valve operation. For example, it is

commonly known that the flow characteristic curves can be altered significantly by manipulating the opening and closing motion of valve plugs. The discrepancies in valve performance between steady state valve coefficient curves and those accounting for valve motion are best characterized in Figure 1. These measurements were taken for the 10-inch LOX service valve operational at Stennis Space Center. Here a large deviation is observed between the steady state mass flow rates and those measured during a timed opening cycle from a plug position of 8.76% open to that of 48% open for a given pressure differential. Furthermore, as the valve reaches the 48% open position, the C_v attains a steady state value after a certain characteristic time depending on the valve geometry and the piping system. A similar albeit smaller deviation in C_v is observed in valve operation during the valve closing cycle. This is not surprising given that the valve was operated in smaller discrete steps of 10% during the closing cycle. At each stage, a sharp gradient in C_v is observed as the mass flow rate/pressure differential settle to the steady state value over some period of time. Prediction of transient behavior related to valve motion can serve as guidelines for valve scheduling, which can be of crucial importance in the rocket engine and component testing environment.

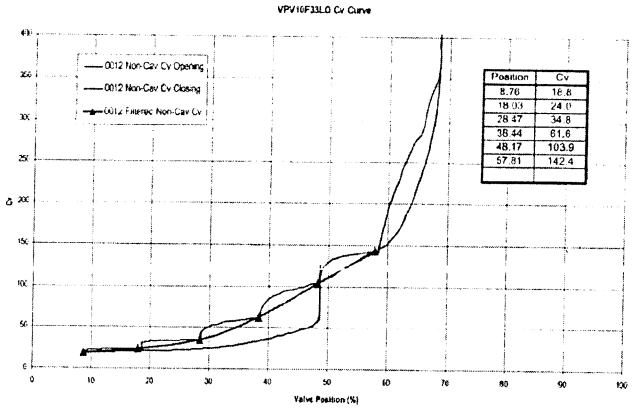

Figure 1. Valve Timing Data for 10-inch LOX Service Valve Operating with Cold Flow (Source: Stennis Space Center).

The operation and testing of rocket engine components/systems is constantly subject to flow induced instabilities and large scale pressure fluctuations. Computational simulations can play an integral role in supporting testing and developmental activities by identifying and characterizing these instabilities. However, in valve and feed systems such instabilities can range from turbulent pressure fluctuations due to vortex shedding from bend and elbows of the piping system, transient effects due to valve scheduling, to large scale fluctuations due to collapse of vapor cavities related to cavitation in inducers and flow control elements such as venturis. The diversity of flow regimes and instability mechanisms place very stringent requirements on any computational framework that could be used for such analyses. For example, the identification of dominant frequencies associated with flow instabilities in such systems requires high order numerics, advanced turbulence modeling capabilities, sophisticated grid topologies to resolve local physics in complex geometries, embedded models for unsteady cavitation, capture thermal effects in cryogenic fluids, and dynamic handling of valve motion. In this paper, we utilize our multi-element unstructured framework that comprises the CRUNCH CFD® code with advanced cavitation, turbulence modeling and grid motion capabilities to simulate the different types of instabilities seen in valve/feed systems – we will classify these instabilities as (a) hydrodynamic instabilities stemming from inherent structural causes (b) dynamic events related to timing of valve motion and (c) cavitation related instability mechanisms in cryogenic flow regimes.

In the past, we have tailored our multi-element unstructured CFD solver to carry out simulations of complex valve and feed system components [3,4]. Computational analyses have been performed for a variety of structurally complex valve systems such as the pressure regulator valve, split body valve and cavitating flow control elements. We have also extended our multi-element unstructured framework to include timing studies for transient valve operation by including valve movement and capturing the flow instabilities associated with it. The distinguishing feature of grid motion in internal flows such as valves from that seen in external aerodynamic type flows is that the topological and physical requirements of the grid can change substantially in localized regions of the flow domain as a result of the grid/valve motion. A valve

operating at a 10% open setting has very different flow physics from one operating at 80% open position. Our approach accounts for this change in grid topology through a unique methodology of mesh movement to accommodate the translating valve.

Cavitation related instabilities are endemic in liquid rocket feed systems and test facilities. Since these flow regimes primarily consist of cryogenic fluids that operate in close proximity to the critical temperature, there are substantial thermal effects and property variations associated with such flows. Our cavitation models account for the coupling of thermodynamic processes with the cavitation processes and have accurately captured such effects as leading edge pressure and temperature depression due to evaporative cooling, and frothy cavitation zones that are the hallmark of cavitated regions in cryogenic fluids. Furthermore, with the incorporation of an unsteady cavitation model we are able to predict amplitudes and frequencies of dynamic pressure loads and track bubble clouds sheared off cavities due to the interaction of reentrant jets in the cavity closure region.

The multi-element unstructured philosophy is discussed in section II along with a control valve example. This control valve experiences valve stall as a consequence of a fluid dynamic instability accompanied by resonance in the plug cavity. In section III, we provide details of mesh movement along with some results for a dynamic control valve used at NASA SSC. In section IV we show results for a cavitating instability for feed system components used in the test facility at NASA SSC.

MULTI-PHASE UNSTRUCTURED METHODOLOGY FOR UNSTEADY VALVE SYSTEM APPLICATIONS

The multi-element unstructured framework has been fine tuned to efficiently solve flows for valve system applications with structurally complicated geometries, cryogenic and real fluid effects, and flow structures that include flow separation, turbulence and intermittency. In a nutshell, the multi-element unstructured philosophy is encapsulated in CRUNCH CFD® code, wherein an optimal combination of tetrahedral, prismatic, pyramidal and hexahedral cells are used to efficiently solve flows in complex systems by tailoring the mesh to suit the geometrical and physical characteristics of the system. In valve systems, in particular, the seat region around the plug is meshed with high aspect ratio hexahedral cells, allowing resolution of large local pressure and velocity gradients. The inlet and discharge ducts of a valve system are meshed with a combination of hexahedral and prismatic layers that help in resolving boundary layer phenomena and the transport of flow structures emanating from the seat region. The mesh in the seat region is typically stitched together with the grid in the inlet and discharge ducts with the aid of tetrahedral domains that provide topological flexibility with structurally complex shaped systems. The strategy has proven to work very efficiently for simulations of a variety of valve systems in use at SSC such as the 10-inch LOX valve, Split-Body valve, Pressure Regulator valve, and the Globe valve (See Ref. Ahuja et al. [3], Shipman et al. [5]). The simulations with the multi-element unstructured CRUNCH CFD® code have yielded results where the flow coefficients have been in excellent agreement with experimental/testing data. Furthermore, this strategy of simulating flows in valve systems has provided key insights into dominant flow physics during valve functioning and testing.

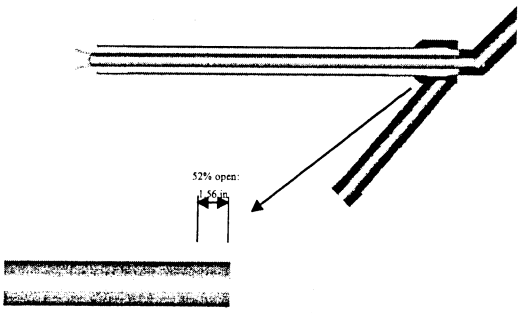

Figure 2. Schematic of the 6 inch Gaseous Hydrogen Valve.

As an illustration of the applicability of the multi-element unstructured framework to valve systems of interest to SSC, we discuss analysis work done on the 6-inch gaseous hydrogen valve (see Figure 2) currently in operation. This

particular system is interesting, both, for the structural complexity in the valve geometry, particularly in the seat region and wide array of physical flow phenomena and flow regimes involved. Furthermore, at testing the valve stalled at a stroke setting close to 52%. CFD Analyses of the flow path at the constant valve setting position helped reveal details of the flow physics and the resultant integrated force balance on the plug. A 3-D multi-element grid has been generated for this 6-inch valve configuration based on the strategy discussed above. Following our standard strategy for complex valve systems, structured domains are constructed around the plug and in the narrow clearances of the seat region. Figure 3 depicts the grid along the plane of symmetry clearly showing the hexahedral blocks in seat region around the plug. Hexahedral/prismatic cells are extruded along the inlet and exhaust pipes and a tetrahedral block used to fill in the junctions between the pipes and the seat. The extruded hexahedral-prism blocks in the inlet and discharge ducts are also shown to interface with a region of tetrahedral cells [3]. This transition from hexahedral to tetrahedral cells permits flexibility in local resolution in different parts of the flow domain.

Simulations of the 6-inch gaseous hydrogen valve were performed with an inlet pressure of 5710 psi and inlet stagnation temperature of 530 R. Our simulations indicate an inlet Mach number of 0.11 with a peak Mach number close to 2.8 in the valve seat. The Mach number distribution is shown in Figure 4 indicating flow expansion with the sudden change in area in the valve seat region. The pressure distribution (shown in Figure 5) also shows the formation of alternate bands of expansion and compression waves. Furthermore, the stream traces plotted in Figure 6 indicate a three-dimensional complex flowpath in the exhaust duct – the incoming jet through the valve seat is unable to negotiate the bend in the exhaust duct leading to the formation of large secondary flow region. The instantaneous Mach number and pressure snapshots shown in Figures 4 and 5 are 1.5e-4 seconds apart and indicate that the cavity in the plug does not represent a benign flow region as is generally the case in such valve configurations. In this case, the cavity acts as a resonance tube with pressure waves from the cavity periodically interacting with the flow in the seat region. This in turn, breaks the symmetry of the flow near the seat region and leads to variable loads on the plug (Figure 7).

Numerical pressure probes were inserted in different parts of the flow domain and the pressure traces were recorded. A Fourier analyses of the traces revealed that globally the fundamental tone of 257 Hz associated with the cavity is seen to play a significant role in exciting the flow in the valve housing. However, there are other significant high-frequency tones associated with the dynamics of the jet through the valve seat that are excited in the valve housing. The unsteadiness in the valve housing is seen to dynamically influence the load on the plug. The time history of the axial force on the plug is plotted in Figure 7. Each count on the x-axis is 10 time iterations or $2x10^{-6}$ seconds and portions above the 12,000 lbf on the y-axis are colored indicating that the force on the valve plug has exceeded the force rating on the actuator, which would cause the valve to stall. The figure shows dramatic fluctuation in the force of more than 3000 lbs and explains the valve stall seen during testing.

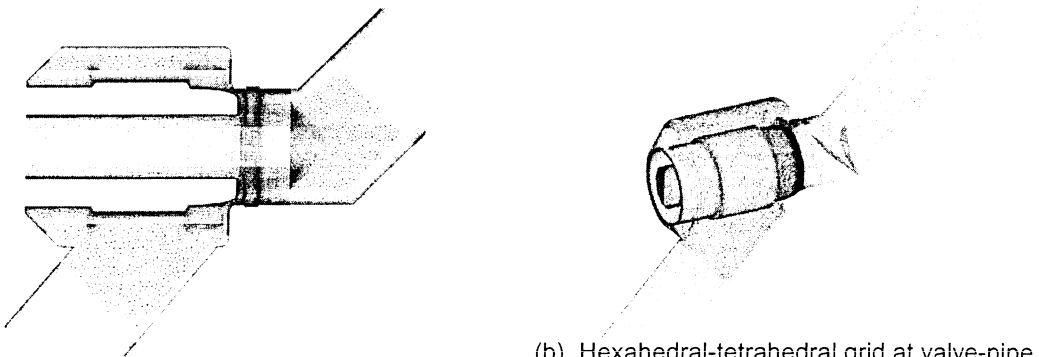

(a). Blow-up of the grid in the seat region

(b). Hexahedral-tetrahedral grid at valve-pipe interface

Figure 3. Multi-Element Grid for the 6 inch Gaseous Hydrogen Valve.

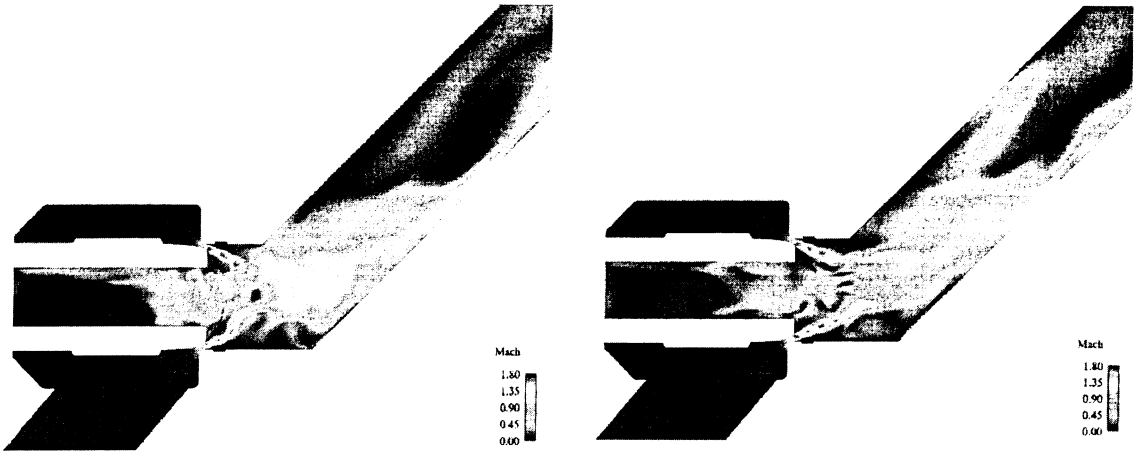

Figure 4. Instantaneous Mach Number Distribution in 6-inch gaseous Hydrogen Valve.

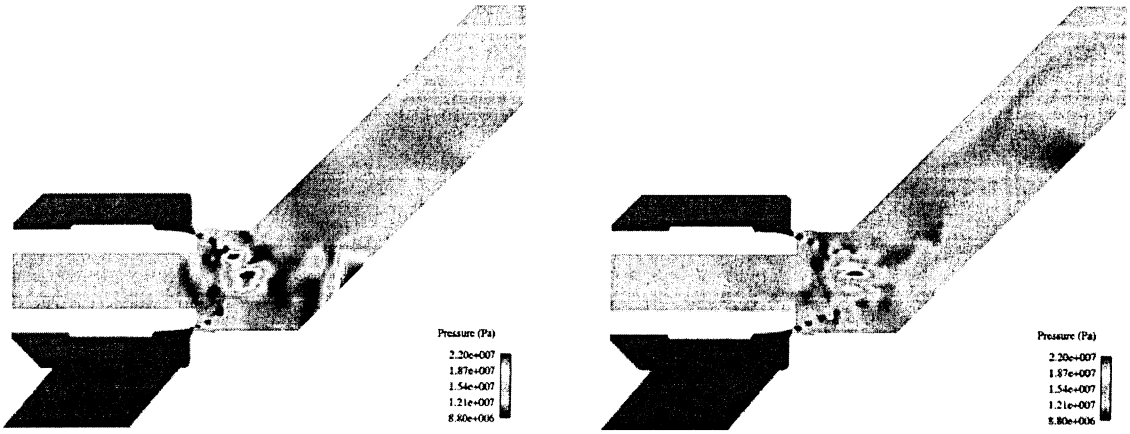

Figure 5. Instantaneous Pressure Distribution in 6-inch gaseous Hydrogen Valve.

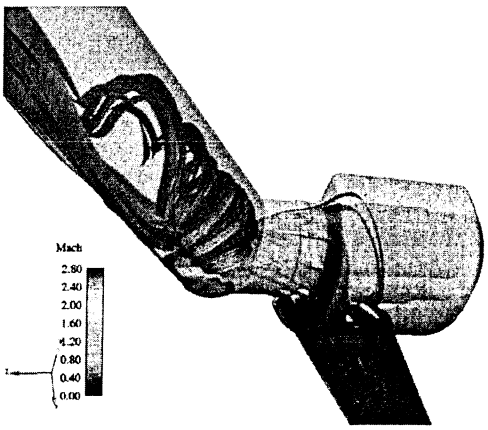

Figure 6. Recirculation Patterns in the discharge duct of the 6-inch Gaseous Hydrogen Valve.

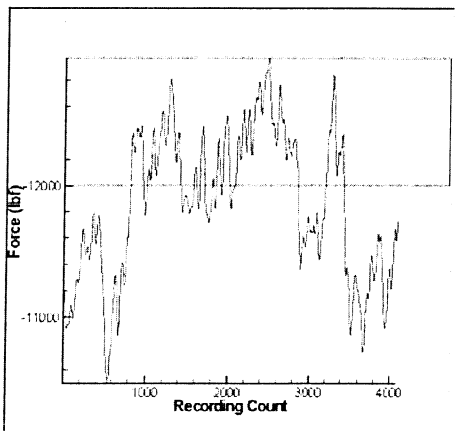

Figure 7. History of the axial force on the plug. (1 unit on the x-axis is 10 time iterations or 2 x 10^{-6} seconds).

TRANSIENT STUDIES RELATED TO VALVE TIMING

In this section we present moving valve simulations working with a unique strategy for valve motion that permitted the use of different grid topologies as the valve opens/closes. Our strategy for valve motion entails making a library of grids for every 10% of change in plug setting and use a generalized mesh motion solver to translate between successive recorded plug setting meshes in the library. This is primarily done because it addresses two important problems: firstly flow paths at lower plug settings such as 5% open are very different from flows at 95% open. Resolution requirements for capturing essential flow gradients are very different and very different multi-element meshes are needed to fulfill the disparate flow resolution criteria. Secondly, a single mesh would undergo tremendous skewness through the entire translation process of the plug, thereby degrading the accuracy. The library of grids would be generated in an automated manner through a scripting process in GRIDGEN [7]. Our scheme models the computational mesh as an elastic solid subject to the equations of elasticity. Any movement of the mesh boundary results in the propagation of a stress through the domain, producing motion of the interior grid points [6]. The current formulation is edge-based and therefore applicable to arbitrary unstructured meshes composed of any combination of tetrahedra, pyramids, prisms, or hexahedra. Details of the grid movement procedure such as prescription of the valve displacement curves, mesh movement scheme, creation of mesh libraries are not dealt here and the reader is referred to an associated publication [8].

In this section we discuss the axisymmetric split-body valve simulations using our mesh movement approach. To accurately model the moving valve problem, the upstream boundary condition had to be modified for incorporation of a variable mass inflow boundary condition. Therefore a stagnation pressure boundary condition is imposed at the inflow. Furthermore, we track critical parameters such as the valve flow coefficient, upstream and downstream pressures and mass flow rates to ensure that the simulation closely mimics the valve behavior. We operate the valve by opening it from a plug position of 40% to a position of 80%. The valve is opened at a constant velocity of 10 inches/sec and an initial mass flow rate of 60lbm/sec. Figure 8 shows a series of instantaneous pressure and velocity distributions in approximately 10% increments. As expected the pressure gradient in the seat relieves itself as the valve progressively opens. Interestingly, the sequence of velocity distributions show the change in flow patterns in the seat region – the intensity of the jet that emanates from the inflow duct decreases as the valve opens. As a consequence, the jet spreads out further (in the radial direction) in the discharge duct and the reattachment length of the corner re-circulation zone in the discharge duct shortens. In Figure 9, we present the grid with the velocity distribution at plug positions of 50%, 60%, 70% and 80%. It can be seen that the flow gradients smoothly transition between the different grid elements and on the distorted grid during grid motion where maintaining flow accuracy is important for such dynamic/transient calculations. The different library meshes are evident by noting the changing location of the hexahedral regions.

The mass flow variation as a function of plug opening for two different plug speeds is plotted in Figure 10(a-b). Figure 10(a) shows the change in mass flow for a plug speed of 10 inches/sec whereas Figure 10(b) corresponds to a slower plug speed of 1 inch/sec. The mass flow variation in Figure 10(a) shows a linear curve in contrast to the mass flow variation in Figure 10(b) where the increase in mass flow closely approximates the variation in plug profile which in turn directly affects the area increase in the seat region. Although both the curves in Figure 10 show a monotonic increase in mass flow, Figure 10(b) indicates that the rate of mass flow increases substantially faster in the case of slower plug velocity. For example, at 45% open, the mass flow through the valve is already at 70 lbs/sec in the case of plug moving at 1 inch/sec whereas the faster plug traveling at 10 inches/sec indicates a mass flow rate of 65 lbs/sec at the same plug setting. The difference in valve performance can be better understood by comparing the flow coefficient curves (Cv) for the two cases. Figure 11 shows a comparison of the variation of Cv with valve opening for the two cases along with Cv variation for quasi-steady calculations performed at discrete plug settings that are 10% apart. It is seen here that the dynamic Cv curve for the 1 inch/sec plug velocity simulation closely matches the data for the quasi-steady simulations, whereas the Cv curve for the faster plug velocity lags the quasi-steady data

indicating the mass flow rate does not respond fast enough to valve opening at higher plug speeds. The effect of valve speed on system response is critical in valve scheduling for efficient engine operation and controlling deleterious fluctuations from impacting component performance.

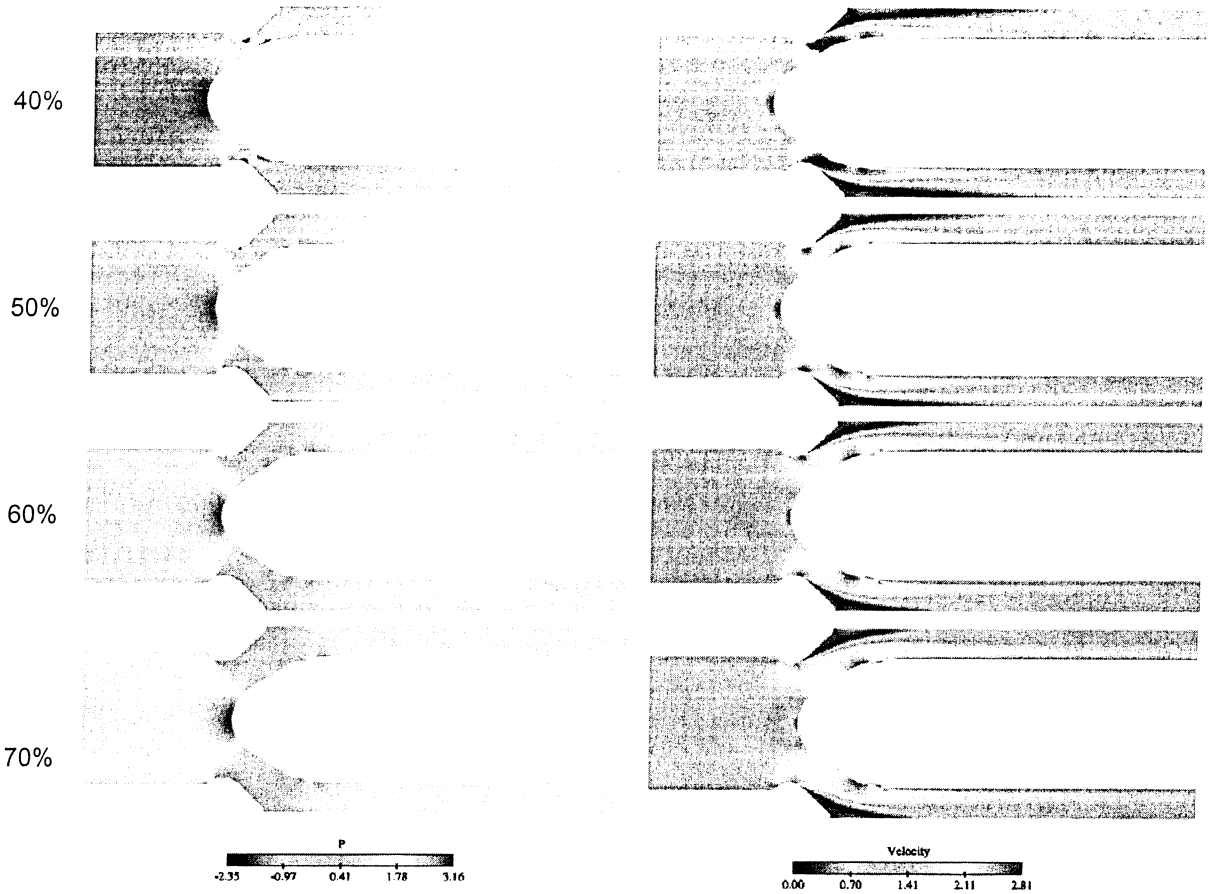

a) Pressure contours b) Velocity contours

Figure 8. Split-Body Valve results at 10% intervals using the library approach.

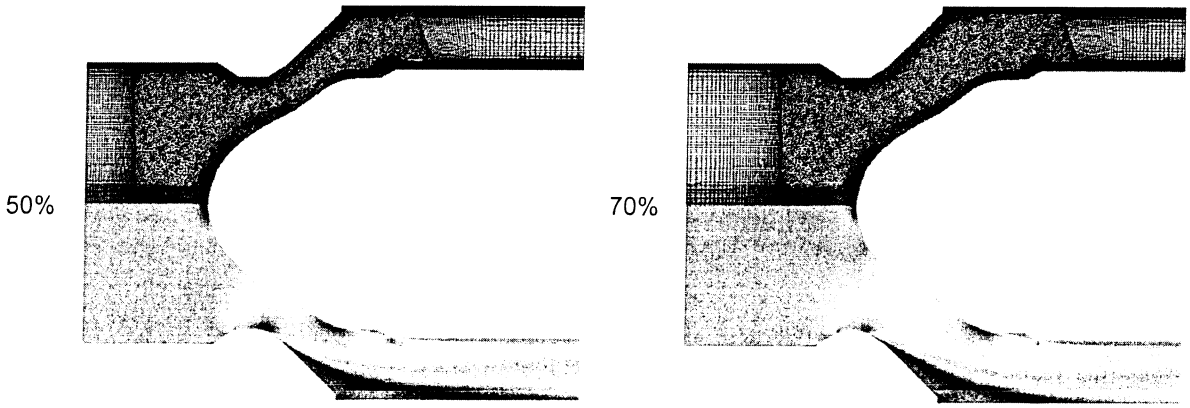

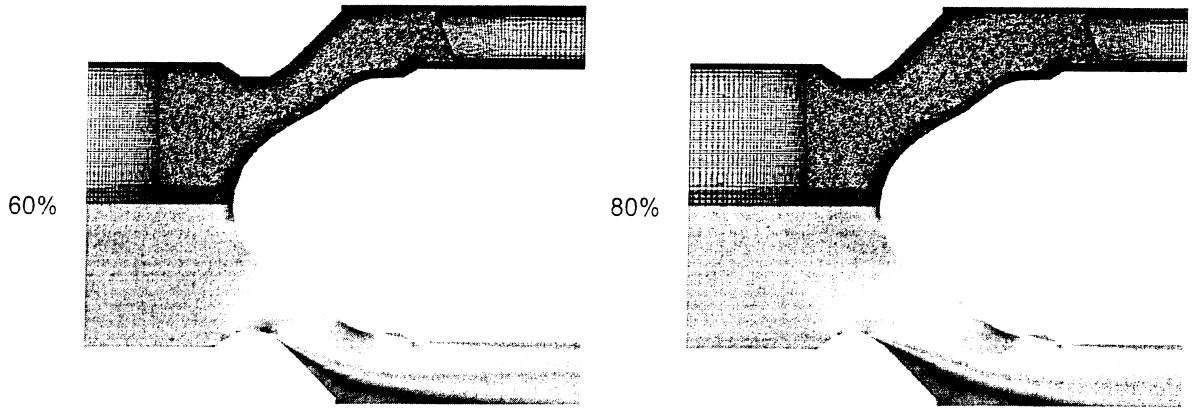

Figure 9. Library meshes for Split-Body Valve simulation.

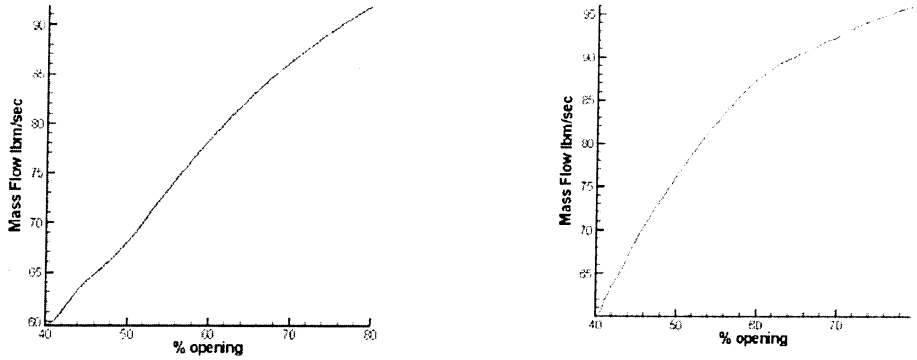

a) Mass flow variation with valve opening at plug speed of 10 inches/sec

b) Mass flow variation with valve opening at plug speed of 1 inch/sec

Figure 10. Performance of Split-Body Valve during opening.

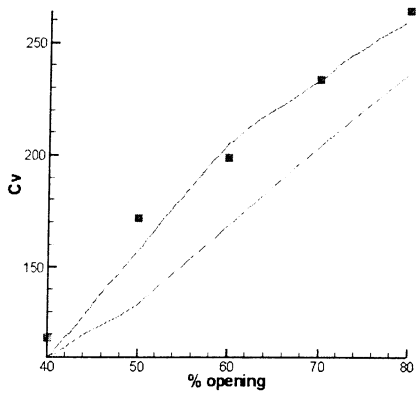

Figure 11. Performance of Split-Body Valve showing flow coefficient as function of valve opening.

CAVITATING INSTABILITIES IN FEED SYSTEM COMPNENTS

In this section, we will discuss the development of cavitating instability in two different feed system components: (a) orifice and (b) flow control venturi that is attached to a 90 degree turning duct. These two components represent the two disparate regimes of cavitating flows: the orifice is representative of traveling cavitation class of flows commonly observed in tip vortices of propeller blades, whereas the venturi represents a sheet cavitation type problem with periodic shedding of vaporous clouds from this well developed cavity.

CAVITATION FROM AN ORIFICE

An orifice is routinely used in testing facilities to step down the pressure and in this section we analyze the cavitating instability that sets up in the testing facility (NASA SSC) due to a pump discharge orifice. The flow rate of liquid hydrogen through the orifice is 130 lbs/sec at an operating temperature at 21.7 K. The inlet pipe has a diameter of 6 inches and the orifice throat diameter is 3.26 inches (with an inlet radius of 0.75 inches). A back pressure corresponding to 65 psia is maintained on the outlet end of the configuration and the corresponding vapor pressure of liquid hydrogen at the operating temperature is 21.755 psia. A snapshot of the instantaneous axial velocity distribution is shown in Figure 12(a), which indicates the formation of a primary jet as flow accelerates to negotiate the orifice. It should be noted that this jet is representative of a very high Reynolds Number flow since cryogens such as liquid hydrogen typically have very low viscosity. Figure 12(b) shows the vorticity associated with the fringes of this jet and Figure 12(c) depicts a snapshot of the pressure distribution. Vorticity production at the lip of the orifice leads to

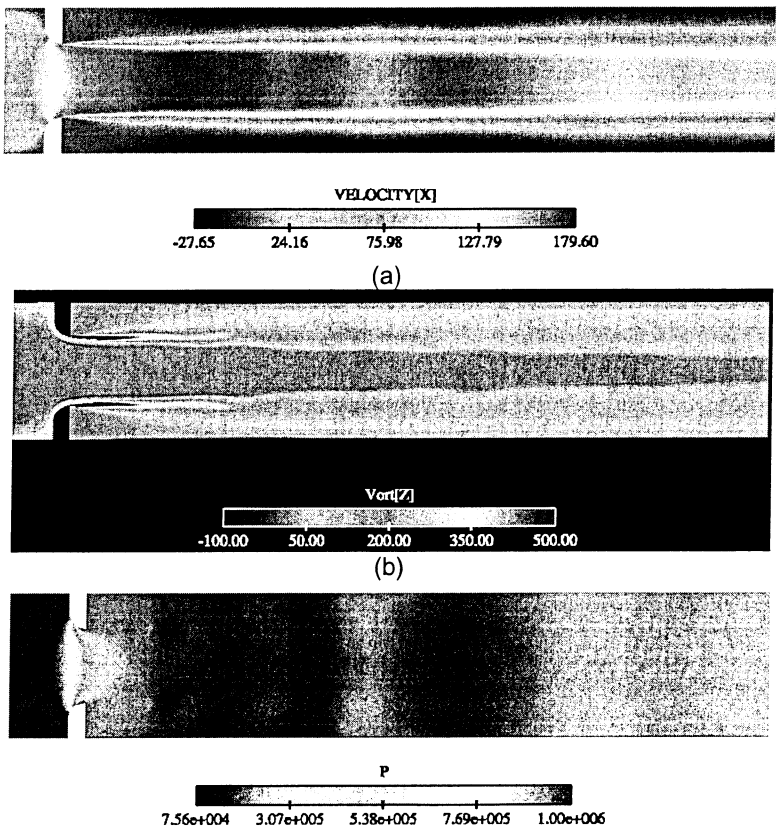

Figure 12. Instantaneous snapshots of (a) axial velocity distribution (b) vorticity distribution and (c) pressure distribution for flow through an orifice.

unsteady shedding and the periodic formation of pockets of low pressure. When the pressure in these pockets falls below the vapor pressure cavitation sets in leading to the formation of a vapor cloud that grows and convects downstream Figure 13).

The shedding of the vapor clouds is a fairly periodic phenomenon as evidenced by the instantaneous void fraction distribution seen in Figure 13. Furthermore, these clouds are formed in regions of high vorticity in the shear layer associated with the primary jet. The growth and development of the vapor clouds be better explained by the sequence of instantaneous void fraction contour plots in a blown up region around the orifice (Figure 14). Here, we see a small cavity formed at the lip of the orifice with a well-defined gas-liquid bubbly wake. As the wake encounters a region of low pressure downstream of the orifice, it leads to sudden expansion and growth of the vapor cloud. Figure 15 shows the pressure traces of two numerical probes located 5 inches and 10 inches downstream of the orifice along the piping wall. Both probes show large scale pressure fluctuations attributed to the highly dynamic processes of formation and collapse of the vapor clouds. The frequency spectrum of the pressure oscillations indicates a cavitation shedding frequency of 80 Hz is excited in both probes with significant energy in a higher overtone of 320 Hz.

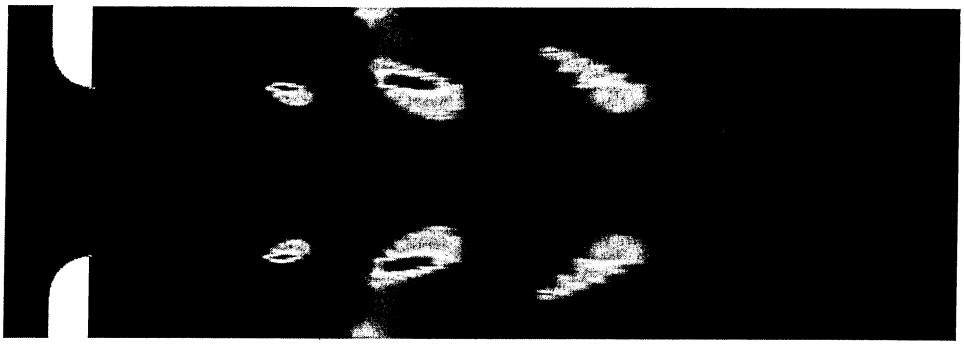

Figure 13. Instantaneous snapshot of vapor void fraction showing shedding of vapor clouds.

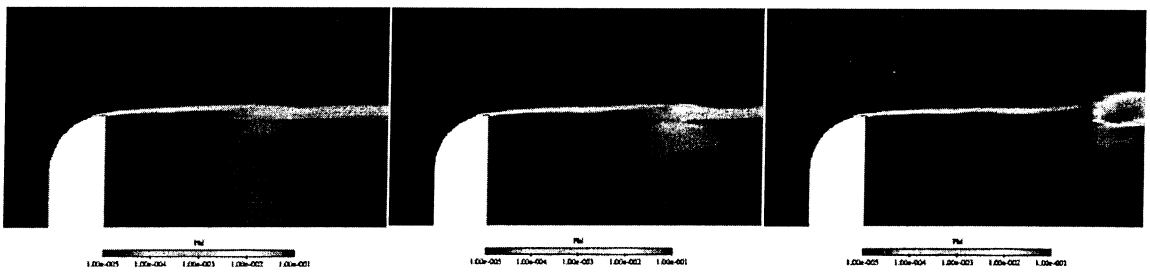

Figure 14. Instantaneous snapshot of vapor void fraction showing formation of cavitation clouds in a blown up region near the orifice.

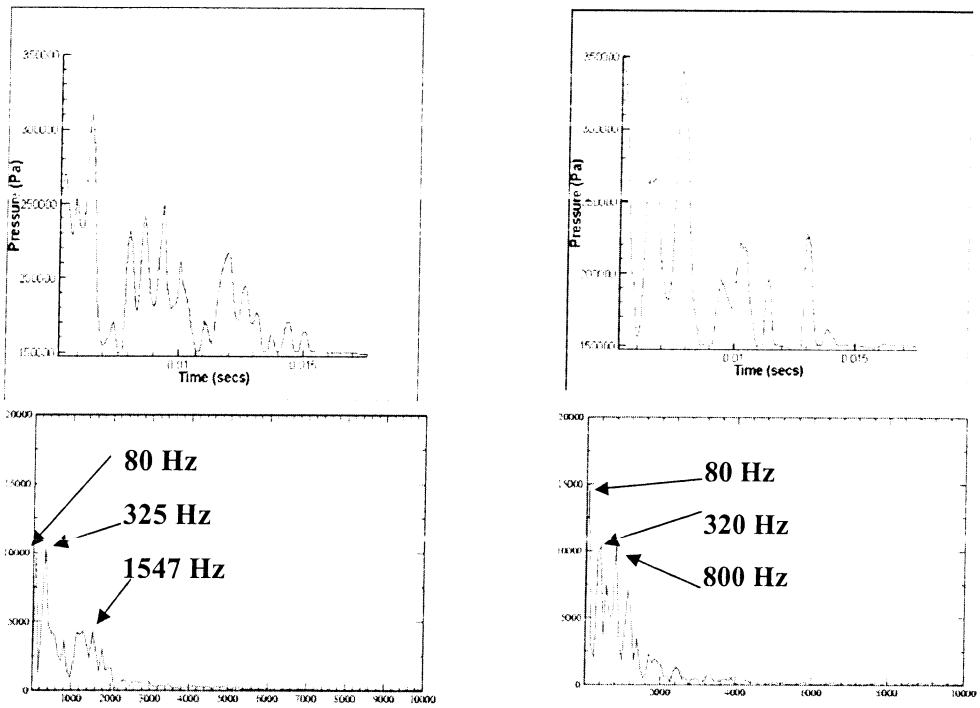

(a) 5 inches downstream of orifice **(b) 10 inches downstream of orifice**

Figure 15. Pressure history and Fourier Decomposition.

CAVITATION IN A VENTUR TURNING DUCT SYSTEM

The venturi is primarily used as a flow control device in various propulsive applications and test facilities. The simulations discussed in this section relate to a cavitating venturi in a LOX feedline that is connected to a 90 degree turning duct. This particular venturi has a throat diameter of 2.94 inches and an inlet diameter of 10 inches. Simulations have previously been carried out by the authors for the case of the standalone venturi. In this case, the calculated discharge coefficient (0.96) compared favorably with the experimental discharge coefficient (0.95). The coupled turning duct and venturi simulations were performed primarily to look at dynamic effects in the system and understand the associated physics. For computational tractability a 2-D configuration of the system was assumed as a half-plane 3-D assumption is not possible due to the presence of the turning duct. The freestream conditions for this case consisted of a freestream velocity of 33.06 m/s and a density of 1132.12 kg/m^3 at a temperature of 92 K. The vapor pressure at the freestream temperature corresponded to 17.69 psi. A sequence of instantaneous void fraction distributions are shown in Figure 16 that depict the process of breakup of the sheet cavity that forms along the walls of the venturi and consequently the convection of the vapor clouds. It should be noted that the asymmetry of the cavitated zones along the upper and lower walls of the cavity is a direct consequence of the coupling between the venturi and the turning duct. A strong reentrant jet develops in the closure region of the cavity that shears large vapor clouds and results in the oscillation of the cavity length.

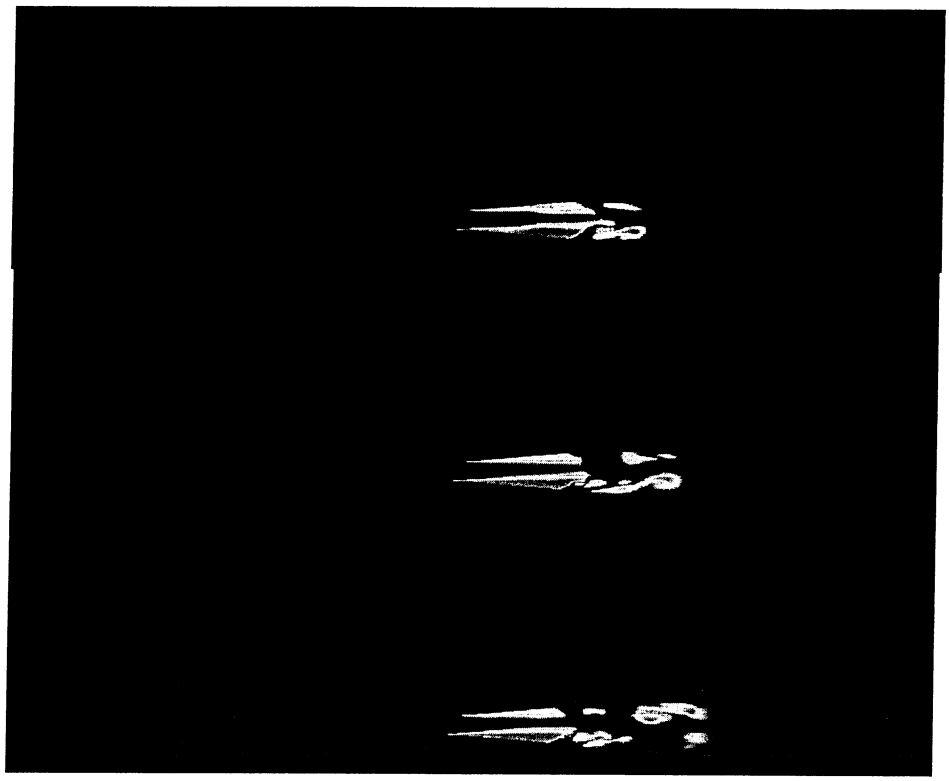

Figure 16. Instantaneous snapshot of vapor void fraction showing shedding of vapor clouds.

An instantaneous snapshot of the pressure distribution (Figure 17) in the system reveals a highly dynamic pressure field both in the turning duct (near the bend) and in the venturi(in the cavity closure region). Pronounced thermodynamic effects that are characteristic of cavitating regimes in cryogenic fluids can be seen in the instantaneous temperature distribution snapshot (Figure 18). Evaporative cooling effects that result in a temperature depression at the leading edge of the cavity can be clearly seen here. Furthermore, we find that the temperature in the core of the vapor clouds that are shed off the main sheet cavity is also significantly lower than the freestream temperature. Such strong temperature (and consequently, vapor pressure) depressions have the potential for creating condensation fronts leading to large pressure excursions and a highly dynamic flowfield. The spectral content of two numerical probes (one downstream of the bend, other downstream of sheet cavity region) show very different excitation frequencies. The probe in the turning duct shows a low frequency dominant mode (100 Hz) related to unsteadiness associated with boundary layer separation along the inner wall just aft of the 90 degree bend with pressure oscillations of about 10%. In contrast, the probe in the venturi shows significant energy in higher frequencies (476 Hz primary excitation mode) and large scale pressure fluctuations (Figure 19).

Figure 17. Instantaneous pressure distribution in the turning duct venturi system.

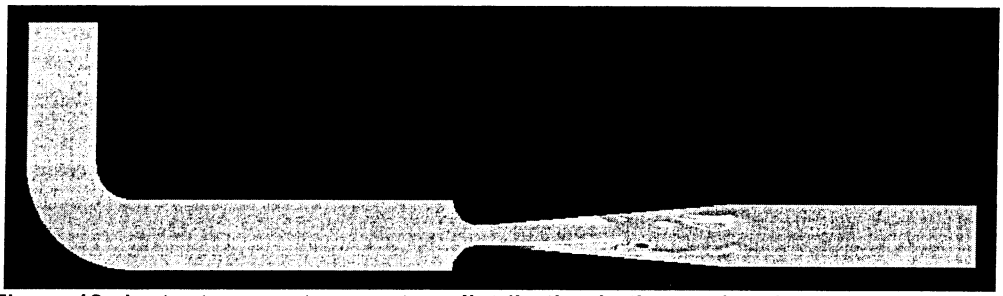

Figure 18. Instantaneous temperature distribution in the turning duct venturi system.

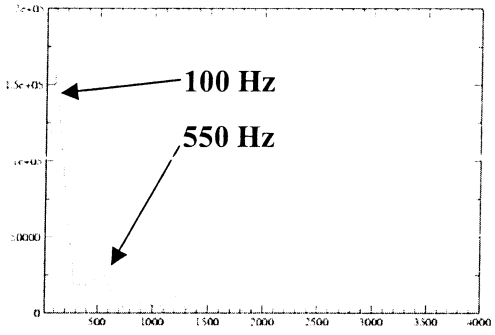

(a) Numerical probe in turning duct downstream of bend

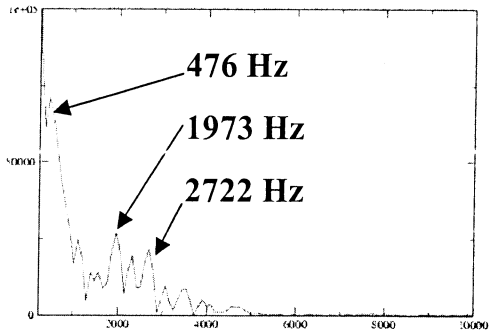

(b) Numerical probe in venturi aft of the sheet cavity

Figure 19. Frequency Spectra for numerical probes in the turning duct venturi system.

SUMMARY AND CONCLUSIONS

An advanced computational tool has been developed to carry out high-fidelity unsteady analyses of valve and feed systems. Our numerical framework utilizes a multi-element unstructured methodology with embedded models for mesh motion, cryogenic cavitation and unsteady bubble dynamics. Such a framework is particularly suited to resolving the different classes of flow induced instabilities and dynamic events in complex systems that can range from hydrodynamic instabilities due to structural complexities and transients due to valve motion to cavitation related instabilities in cryogenic regimes with significant thermodynamic effects. In this paper, we have shown the versatility of our computational framework by carrying out detailed numerical simulations for problems from each sub-class of transient problems related to valve and feed system a complex control valve configuration that exhibits valve stall; valve scheduling for the split body valve; and transient cavitation problems for two different systems components i.e. orifice used to step down pressure and a venturi-turning duct system. Numerical simulations of the control valve revealed the physics behind the valve stall related directly to flow resonance in the plug cavity. Large flow gradients that set up in the seat region were accurately captured and the unsteady interaction between the between flow in the plug cavity and the jet structure in the seat region creates unsteady loads that were shown to be greater than the actuator force rating on the plug leading to valve stall.

Unsteady simulations of valve timing for the split body valve were carried out utilizing a novel moving grid approach that permits the use of variable grid topology by maintaining a library of high-fidelity meshes and dynamic mesh motion via mesh deformation between the adjacent library meshes. The split body valve simulation undergoes valve motion from a 40% open plug position to a 80%open position through a succession of four library grids. The solutions evolve smoothly through the simulation process and the valve coefficient at lower plug speeds compares favorably with quasi-steady simulation data. Furthermore, we show that at higher plug speeds the

valve does not respond fast enough to plug motion. Dynamic flow coefficient curves such as the ones obtained during our transient simulations are very valuable for testing purposes because it can help in improving valve scheduling on test stands and predicting unsteady phenomena such as valve stall.

Unsteady cavitating simulations were also performed for two different components regularly used in test facilities: step down orifice and a coupled turning duct venturi system. Both simulations were performed for cryogenic fluids (liquid hydrogen and liquid oxygen) in flow regimes where termodynamic effects are significant. Simulations of the orifice show a periodic shedding of vapor clouds from the lip of the orifice and the formation of these clouds is directly linked to vorticity production from the orifice. Furthermore, fundamental frequencies associated with the cavitation shedding process were captured as part of the simulation process and could provide valuable insight to testing facilities. Simulations were also performed for a coupled turning duct venturi system operating in liquid oxygen. Here, the dynamic process of formation, shedding and convection of large scale vapor clouds in the venturi was captured as part of the simulation. Furthermore, these simulations showed a strong coupling between thermodynamic effects and the cavitation process with temperature depression at the leading edge of the cavity and in the core of vapor clouds shed due to the interaction of the reentrant jet and the cavity. Frequency spectra of probes in the turning duct and the venturi indicates very different modes are excited in the disparate parts of the system. Vortex shedding from the bend in the turning duct is responsible for small amplitude low frequency excitation whereas a high frequency excitation causing large scale fluctuations is seen in the venturi primarily due to the cavitation shedding and condensation process.

ACKNOWLEDGMENTS

We acknowledge funding for this work through a NASA SBIR, Contract Number NNS04AA08C funded by NASA Stennis Flight Center. Dr. Peter Sulyma was the technical monitor and his input is gratefully acknowledged.

REFERENCES

1. Daines, R.L., Woods, J.L., and Sulyma, P.R., "Computation Analysis of Cryogenic Flow Through a Control Valve," FEDSM2003-45120, 4th ASME-JSME Joint Fluids Engineering Conference, Honolulu, Hawaii, July 2003.
2. Miller, D.S., "Internal Flow Systems," BHRA Fluid Engineering, 1978.
3. Ahuja, V., Hosangadi, A. and Shipman, J., "Multi-Element Unstructured Analyses of Complex Valve Systems," 52nd JPM/1st LPS Meeting, Las Vegas, NV, May 10-14, 2004.
4. Ahuja, V., Hosangadi, A. and Shipman, J., "Computational Analyses Of Cavitating Control Elements In Cryogenic Environments," Paper No. HT-FED2004-56377, The 2004 Joint ASME-JSME Fluids Engineering Summer Conference, Charlotte, N.C., July 11-15, 2004.
5. Shipman, J., Hosangadi, A., and Ahuja, V., "Unsteady Analyses of Valve Systems in Rocket Engine Testing Environments," Paper No. AIAA-2004-3663, 40th AIAA/ASME/SAE/ASEE Joint Propulsion Conference and Exhibit, Fort Lauderdale, FL, July 11-14, 2004.
6. Cavallo, P.A., Sinha, N., and Feldman, G.M., "Parallel Unstructured Mesh Adaptation for Transient Moving Body and Aeropropulsive Applications", AIAA Paper 2004-1057, 42nd Aerospace Sciences Meeting and Exhibit, Reno, NV, January 5-8, 2004.
7. Gridgen, Grid Generation Software Package, Ver. 15, Pointwise, Inc., Ft. Worth, TX, 2004.
8. Cavallo, P.A., Hosangadi, A., and Ahuja, V., "Transient Simulations of Valve Motion in Cryogenic Systems", AIAA Paper No. 2005-5152, 35th Fluid Dynamics Conference and Exhibit, Toronto, Canada, June 2005.